

UNIVERSITY of CALIFORNIA
SANTA CRUZ

**TWO-DIMENSIONAL MODELING OF DOUBLE-DIFFUSIVE
CONVECTION IN THE PRESENCE OF AN EXTERNAL
MAGNETIC FIELD**

A thesis submitted in partial satisfaction of the
requirements for the degree of

BACHELOR OF SCIENCE

in

ASTROPHYSICS

by

Ariel Eileen Kellison

June 2010

The thesis of Ariel Eileen Kellison is approved by:

Professor Gary Glatzmaier
Advisor

Professor David P. Belanger
Senior Theses Coordinator

Professor David P. Belanger
Chair, Department of Physics

Copyright © by

Ariel Eileen Kellison

2010

Abstract

Two-Dimensional Modeling of Double-Diffusive Convection in the Presence of an External Magnetic Field

by

Ariel Eileen Kellison

The purpose of this thesis is to explicate the development of a two-dimensional numerical simulation created to explore the phenomena of double-diffusive convective instability in the presence of a magnetic field. Two types of double-diffusive instabilities are investigated and explained: finger instability, occurring when an unstable compositional gradient is coupled with a stable temperature gradient, and oscillating instability, occurring when an stable compositional gradient is coupled with an unstable temperature gradient. This work emphasizes the basic theory of the physical system's behavior in a manner which the author hopes will provoke the reader to establish their own predictions regarding the effect of imposing a uniform magnetic field on an electrically conducting fluid within a double-diffusive regime. A copy of both the main numerical simulation developed as well as a code used to construct visualizations is provided.

Contents

Introduction	5
Rayleigh-Bénard Convection	6
Formulation of the Rayleigh-Bénard Convection Model	6
Linear Stability Analysis	10
Double Diffusive Instability	12
Basic Theory	12
Stability Configurations	13
Linear Stability Analysis for Double-Diffusive Regimes	17
Magnetohydrodynamics	19
Governing Equations	19
Imposing a Background Magnetic Field	22
Complete Model	24
Numerical Methods	25
Time Integration	25
Vertical Finite Difference Discretization	27
Horizontal Spectral Decomposition	28
Preparation of Model Equations for Code Implementation	29
Code Flow Chart	32
Results and Concluding Remarks	33
Appendix I: Complete Fortran 90 Code	36
Appendix II: Complete IDL Code for Creating Visualizations	44
Bibliography	47

Introduction

This paper emphasizes the phenomena of magnetohydrodynamical double-diffusive instability in regard to planetary science. The two regimes of double-diffusive instability investigated align with processes existing within the interiors and oceans of planets and their moons. The external magnetic field present could be considered as generated by convection occurring within the objects own interior or one generated by a nearby planet or moon with which the object studied has a significant amount of interaction.

The numerical methods used to simulate magnetohydrodynamical double-diffusive instabilities follow those of Glatzmaier (2010). Numerical simulation is an especially necessary tool for connecting and supplementing the traditional theoretical and experimental approaches to investigating the existence of magnetohydrodynamical processes occurring in planetary systems. It provides a medium in which such humanly irreproducible physical processes can be accurately replicated and researched. Although the numerical simulation created for this project is two-dimensional and therefore cannot be considered a precise model for the occurrence of double-diffusive magnetohydrodynamical instabilities in nature, it does provide valuable information on the basic behavior of such systems.

This paper is organized such that an introduction to the numerical methods used for simulation development proceeds descriptions of Rayleigh-Bénard convection, double-diffusion, and magnetohydrodynamics. Appendix I provides a copy of the main numerical simulation and Appendix II provides a copy of the IDL code used to construct visualizations.

Rayleigh-Bénard Convection

The first experiments exploring the transport of heat by fluid movements, a process known as convection, were conducted by Henri Bénard in 1900. Bénard discovered that there was a precise moment at which convective instability occurred, and that this instability led to the development of hexagonal convection cells, now known as Bénard convection cells. In 1916, intrigued by Bénard's experiments, Lord Rayleigh used linear stability analysis to derive the analytical requirement for the development of convective motion. Rayleigh determined that the condition necessary for the onset of thermal instability, and therefore convection, occurred when the ratio of the destabilizing effect of buoyancy to the stabilizing effect of viscosity exceeded a certain critical value.

A detailed explanation of the Rayleigh-Bénard convection model simulated is given in the following section. Lord Rayleigh's analytic work on the numerical requirement for convection to occur within a fluid is given in the section on Linear Stability Analysis.

2.1

Formulation of the Rayleigh-Bénard Convection Model

The Rayleigh-Bénard convection model adopted is based upon the work of Glatzmaier (2010). The model employs a set of equations and boundary conditions describing the process of thermal convection for a nearly incompressible liquid under a uniform gravitational field within a two-dimensional rectangular domain. The upper and lower boundaries of the domain are isothermal and the side boundaries of the domain are thermally insulating.

Rayleigh-Bénard convection is described by the usual Navier-Stokes equations of hydrodynamics but is made within the Boussinesq approximation. The Boussinesq approximation assumes the fluid considered is incompressible. For a fluid to be considered incompressible the following must be true:

1. Density perturbations occur only due to fluctuations in temperature.
2. The background density profile remains constant in both space and time.

The equation of state for such a system is

$$\tilde{\rho} = \rho_0[1 - \alpha(\tilde{T} - T_0)] \quad , \quad (0.1)$$

where $\tilde{\rho}$ and \tilde{T} represent the sum of reference (given by ρ_0 and T_0) and perturbation values for density and temperature, and α is the coefficient of thermal expansion. The Boussinesq approximation therefore reduces the continuity equation

$$\frac{\partial \rho}{\partial t} + \nabla \cdot (\rho \mathbf{v}) = 0 \quad , \quad (0.2)$$

which is the law of conservation of mass in differential form, to

$$\nabla \cdot \mathbf{v} = 0 \quad . \quad (0.3)$$

The remaining Navier-Stokes equations communicate conservation of internal energy (Eq. 0.4 and momentum (Eq. 0.5);

$$\frac{\partial T}{\partial t} = -(\mathbf{v} \cdot \nabla)T + \kappa \nabla^2 T \quad (0.4)$$

$$\frac{\partial \mathbf{v}}{\partial t} = -(\mathbf{v} \cdot \nabla)\mathbf{v} + \nu \nabla^2 \mathbf{v} - \frac{\nabla p}{\rho_0} + \alpha g_0 T \hat{\mathbf{z}} \quad . \quad (0.5)$$

Advection manifests in terms of the form $-(\mathbf{v} \cdot \nabla) \epsilon$, and terms of the form $\nabla^2 \epsilon$ are representative of diffusion. The viscous and thermal diffusivities, ν and κ respectively, are known constants inherent to the fluid.

Taking the curl of Eq. 0.5 and defining a velocity field $\mathbf{v} = v_x \hat{\mathbf{x}} + v_z \hat{\mathbf{z}}$ produces the vorticity equation, whose only non-zero component in the $\hat{\mathbf{y}}$ direction,

$$\frac{\partial \omega}{\partial t} = [-(\mathbf{v} \cdot \nabla)\omega - \alpha g_0 \frac{\partial T}{\partial x} + \nu \nabla^2 \omega] \hat{\mathbf{y}} \quad . \quad (0.6)$$

Eq. 0.6 states that the Eulerian time derivative of vorticity is equal to the sum of the advection by the flow, vorticity generation by buoyancy and vorticity diffusion by viscosity, respectively.

A significant simplification that helps with both the analytic and theoretical approach to Rayleigh-Bénard convection is the use of non-dimensional variables. Although this can be done in several different ways, the traditional scaling for this problem is to measure the length scale in units of the region's depth (D), time in units of $\left(\frac{D^2}{\kappa}\right)$, temperature in units of the temperature drop across the box (ΔT), and pressure in units of $(\rho_0 \frac{\kappa}{D})$. Scaling in this manner allows for the variables of the problem to be rewritten as

$$\begin{aligned} x &= Dx' \quad , \quad z = Dz' \\ t &= \left(\frac{D^2}{\kappa}\right)t' \quad , \quad v = \left(\frac{\kappa}{D}\right)v' \quad , \quad \nabla = \left(\frac{1}{D^2}\right)\nabla' \\ T &= (\Delta T)T' \quad , \quad p = \rho_0 \frac{\kappa}{D}p'. \end{aligned} \tag{0.7}$$

Introducing transformations 0.7 into Eq. 0.4 and 0.6 and dropping the primes for simplicity results in the non-dimensional set of equations

$$\frac{\partial \omega}{\partial t} = -(\mathbf{v} \cdot \nabla)\omega - RaPr \frac{\partial T}{\partial x} + Pr \nabla^2 \omega \tag{0.8}$$

$$\frac{\partial T}{\partial t} = -(\mathbf{v} \cdot \nabla)T + \nabla^2 T. \tag{0.9}$$

The two non-dimensional constants appearing in Eq. 0.8 are the Rayleigh number (Ra) and Prandtl Number (Pr),

$$Ra = \frac{g_0 \alpha \Gamma D^4}{\kappa \nu}. \tag{0.10}$$

$$Pr = \frac{\nu}{\kappa}. \tag{0.11}$$

Here g_0 is the magnitude of gravitational acceleration, α is the coefficient of thermal expansion, $\Gamma = \frac{-d\tilde{T}}{dz} = \nabla T$, D is the depth of the region. Physically, the Rayleigh number represents the ratio of destabilizing effects due to buoyancy to the stabilizing effect of viscous forces. The Prandtl number is the ratio of viscous to thermal diffusion, and gives an indication of the scale size of flow structures compared to the scale size of thermal structures (Glatzmaier).

The boundary conditions imposed upon equations 0.8 and 0.9 are

Velocity Boundary Conditions

- *Region boundaries are impermeable:*

(perpendicular components of the velocity vanish along region surfaces)

$$v_x = 0 \text{ at } x = 0, L \quad (0.12)$$

$$v_z = 0 \text{ at } z = 0, D. \quad (0.13)$$

- *Region boundaries are stress-free:*

(the rates of tangential strain vanish along region surfaces)

$$\frac{\partial v_x}{\partial z} = 0 \text{ at } z = 0, D \quad (0.14)$$

$$\frac{\partial v_z}{\partial x} = 0 \text{ at } x = 0, L \quad (0.15)$$

Temperature Boundary Conditions

- *Isothermal lower and upper boundaries :*

$$T = 0 \text{ at } z = 0 \quad (0.16)$$

$$T = \Delta T \text{ at } z = D. \quad (0.17)$$

- *Thermally insulating side boundaries :*

$$\frac{\partial T}{\partial x} = 0 \text{ at } x = 0, L \quad (0.18)$$

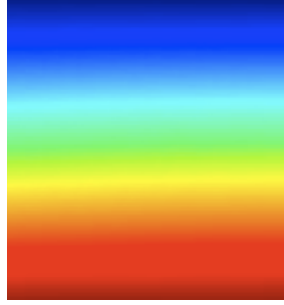


Figure 0.1: A snapshot of the initial temperature profile for the Rayleigh-Bénard convection model described.

2.2

Linear Stability Analysis

Lord Rayleigh's analytic solution of the thermal convection problem is considered to be a major breakthrough in the history of linear stability theory. The Rayleigh number (Eq. 0.10) is a dimensionless constant equal to the ratio of destabilizing buoyant forces promoting convective motion to stabilizing viscous forces working to dampen convective motion. Rayleigh derived what is known as the critical Rayleigh number, whose value represents the point at which buoyant forces become significantly dominant in comparison to viscous forces. *For convection to develop within a given system the Rayleigh number must be appreciably larger than the critical Rayleigh number.*

Rayleigh's derivation of the critical Rayleigh number assumes the representation of the streamfunction, vorticity, and temperature departure as sums of double Fourier components (Saltzman 1962). In concordance with the boundary conditions 0.12 - 0.18, the full Fourier expansion of the temperature, vorticity, and streamfunction are

$$T(x, z, t) = \sum_{n=0}^{N_n} \sum_{m=1}^{N_m} T_{nm}(t) \sin(m\pi z) \cos\left(\frac{n\pi x}{a}\right) \quad (0.19)$$

$$\omega(x, z, t) = \sum_{n=1}^{N_n} \sum_{m=1}^{N_m} \omega_{nm}(t) \sin(m\pi z) \sin\left(\frac{n\pi x}{a}\right) \quad (0.20)$$

$$\psi(x, z, t) = \sum_{n=1}^{N_n} \sum_{m=1}^{N_m} \psi_{nm}(t) \sin(m\pi z) \sin\left(\frac{n\pi x}{a}\right) \quad (0.21)$$

Here n is the horizontal (x) Fourier mode number, m is the vertical (z) Fourier number, and N_n, N_m are the chosen truncation levels in the expansions (Glatzmaier). Reducing the nonlinear advective terms $(\mathbf{v} \cdot \nabla)T$ and $(\mathbf{v} \cdot \nabla)\omega$ to

$$(v_z)_n = \left(\frac{\partial\psi}{\partial x}\right)_n = \left(\frac{n\pi}{a}\right) \psi_n, \quad (0.22)$$

through formulation of the streamfunction ψ

$$\mathbf{v} \equiv \nabla \times (\psi \hat{\mathbf{y}}) = -\frac{\partial\psi}{\partial z} \hat{\mathbf{x}} + \frac{\partial\psi}{\partial x} \hat{\mathbf{z}} \quad (0.23)$$

and utilizing the Fourier expansions 0.19 and 0.21 results in the following linear equations describing the vertical and time dependent Fourier coefficients of temperature, vorticity, and streamfunction ($T_n, \omega_n,$ and ψ_n) :

$$\frac{\partial T_n}{\partial t} = \left(\frac{n\pi}{a}\right) \psi_n + \left(\frac{\partial^2 T_n}{\partial z^2} - \left(\frac{n\pi}{a}\right)^2 T_n\right) \quad (0.24)$$

$$\frac{\partial \omega_n}{\partial t} = RaPr \left(\frac{n\pi}{a}\right) T_n + \left(\frac{\partial^2 \omega_n}{\partial z^2} - \left(\frac{n\pi}{a}\right)^2 \omega_n\right) \quad (0.25)$$

$$\omega_n = -\left(\frac{\partial^2 \psi_n}{\partial z^2} - \left(\frac{n\pi}{a}\right)^2 \psi_n\right). \quad (0.26)$$

Eq. 0.26 follows from the Poisson equation,

$$\omega = \nabla \times \mathbf{v} = \nabla^2 \psi \quad . \quad (0.27)$$

The critical Rayleigh number is the Rayleigh number at which the solution to the system is neither increasing nor decreasing in time, but is instead balanced between forces that work to stabilize and destabilize the system. Therefore, setting the time derivatives in Eq. 0.24 - 0.26 to zero and solving for the Rayleigh number results in an expression for the critical Rayleigh number (Ra_{crit}) for a given aspect ratio and mode number.

$$Ra_{crit} = \left(\frac{\pi}{a}\right)^4 \frac{(n^2 + (am)^2)^3}{n^2} \quad (0.28)$$

3

Double Diffusive Instability

The simultaneous presence of two diffusing components within a fluid leads to the phenomena of double-diffusive convection. The minimum requirements for the occurrence of double-diffusive convection are :

1. The fluid must contain two or more components having different molecular diffusivities. It is the differential diffusion that produces the density differences required to drive the motion.
2. The components must make opposing contributions to the vertical density gradient.

(Turner 1974). The form of the convective motion resulting from the coupling of two diffusive components depends on whether motion is driven by the substance of higher or lower diffusivity.

3.1**Basic Theory**

The stability of a fluid in double-diffusive regimes is dependent upon the configuration of compositional and thermal gradients. The density of the fluid is given by the equation of state

$$\tilde{\rho} = \rho_0[1 - \alpha(\tilde{T} - T_0) + \beta(\tilde{C} - C_0)], \quad (0.29)$$

where the value of α is the coefficient of thermal expansion, determining how fast the density decreases with temperature, and β is the coefficient of compositional expansion, determining how fast the density increases with composition. The values ρ_0 , T_0 , and S_0 represent the reference density, reference temperature and reference composition respectively. Variables with a tilde ($\tilde{}$) represent the combination of perturbation and reference values.

The equations governing double-diffusion are nearly identical to those of Rayleigh-Bénard convection. The inclusion of the advection-diffusion equation for composition and the addition to

the vorticity equation of the term for advection of vorticity due to buoyancy driven by composition are the only changes made;

$$\frac{\partial \omega}{\partial t} = -(\mathbf{v} \cdot \nabla) \omega \pm Pr(Ra \frac{\partial T}{\partial x} \pm Ra_{comp} \xi \frac{\partial C}{\partial x}) + Pr \nabla^2 \omega \quad (0.30)$$

$$\frac{\partial C}{\partial t} = -(\mathbf{v} \cdot \nabla) C + \xi \nabla^2 C. \quad (0.31)$$

The two non-dimensional constants are the compositional Rayleigh number (Ra_{comp}) and Lewis Number (ξ), defined as

$$Ra_{comp} = \frac{g_0 \beta \Gamma_c D^4}{\kappa_c \nu}. \quad (0.32)$$

$$\xi = \frac{\kappa_c}{\kappa}. \quad (0.33)$$

$\Gamma_c = \frac{d\tilde{C}}{dz}$ is the vertical temperature gradient and κ_c is the compositional diffusivity. The compositional Rayleigh number upholds the same representation as the thermal Rayleigh number discussed previously but for the case of composition. The Lewis number is the ratio of compositional to thermal diffusivities, and is generally much less than unity. This relationship is intuitive, as one would expect temperature to diffuse at a rate much faster than that of any compositional element.

3.2

Stability Configurations

The nature of the convective motion generated in a double-diffusive regime is dependent upon whether thermal or compositional diffusive component is promoting the initial instability. The stability configurations available in double-diffusive convection are determined by the sign of the terms describing the advection of vorticity due to buoyancy in the vorticity equation,

$$\pm (Ra Pr \frac{\partial T}{\partial x} \pm \xi Ra_{comp} \frac{\partial C}{\partial x}) \quad (0.34)$$

A system in which the temperature is “top heavy”, implying that the temperature is lowest at the top of the fluid layer, is considered unstable and is defined by a negative temperature gradient $\Gamma = \frac{-d\tilde{T}}{dz}$.

A system which is “top heavy” in composition is also considered unstable, but is defined as having a positive gradient ($\Gamma = \frac{d\tilde{C}}{dz}$), indicating that the composition is highest at the top of the fluid layer. A stable density stratification is one in which the entire system produces a density that decreases with height ($\frac{d\tilde{\rho}}{dz} < 0$). The effect of diffusion in a double-diffusive regime can be to destabilize a stable density gradient, and is therefore fundamentally different than a system containing a single diffusing component in which a stable density gradient implies that no convective motion would occur.

For “top heavy” cases in which $\Gamma = \frac{-dT}{dz}$ the Rayleigh number (Ra) was defined in the section on Rayleigh-Bénard convection as being positive. The Rayleigh number for a system with a positive (stable) temperature gradient is therefore negative. The compositional Rayleigh number (Ra_{comp}) is not subject to this same definition. A positive compositional gradient indicates a positive compositional Rayleigh number, and a negative compositional gradient implies a negative compositional Rayleigh number.

The first of the two configurations of double-diffusive instabilities investigated here involves stable temperature and unstable compositional gradients. Such a configuration indicates that the vertical derivatives of the temperature and composition in the region being considered are both positive. The term describing the advection of vorticity due to buoyancy within the vorticity equation for such a system is

$$-Pr(Ra \frac{\partial T}{\partial x} - \xi Ra_{comp} \frac{\partial C}{\partial x}) \hat{\mathbf{z}} \quad . \quad (0.35)$$

Due to the condition that $\kappa_c \ll \kappa$, a particle displaced in a configuration described by Eq. 0.35 will dissipate heat quickly but will exchange a comparatively inconsequential amount of composition with the surrounding fluid. A parcel of fluid displaced downward will therefore remain heavy in comparison to neighboring parcels due to its steadily decreasing temperature and nearly constant level of composition. A parcel that is displaced upward will remain in a constantly lighter state than its surroundings and therefore continue to rise because it gains heat and remains compositionally light. This behavior leads to the evolution of long narrow convective cells known as fingers, depicted in Fig. 0.2 and 0.3.

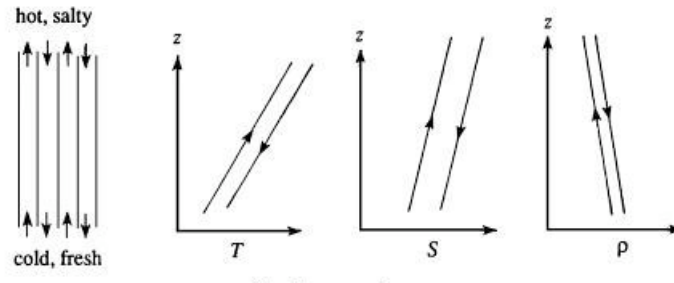


Figure 0.2: Finger Instability, showing up and down going fingers and their temperature, composition (S), and density. Arrows indicate the direction of motion (Kundu & Cohen 2008).

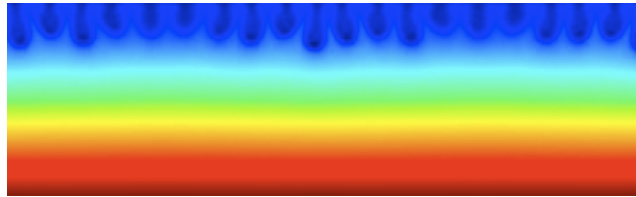


Figure 0.3: An early snapshot of a numerical simulation created by the author in which compositional fingers develop.

Finger Instability, the term used to describe a double-diffusive system in which finger convection cells are produced, occurs within the earth's oceans where the compositional element is due to salt content. Many laboratory observations of salt fingers have been made and shadowgraph images in the deep ocean have confirmed their existence in nature (Kundu & Cohen 2008). Microstructure measurements made by the Caribbean-Sheets and Layers Transects (C-SALT) field program have shown that finger regions in the ocean may be much thicker than would be expected from scaling the results of laboratory experiments to oceanic temperature gradients and salinity steps (Taylor & Bucens 1989).

The Earth's ocean is an electrically conducting fluid, and secondary magnetic fields are generated as it flows through the Earth's magnetic field. In a full magnetohydrodynamic process, a topic that will be addressed in much more detail in the section on magnetohydrodynamics, the electromagnetic fields and the flow of an electrically conducting fluid are coupled. In the ocean,

however, flow generates electromagnetic fields but the electromagnetic fields are not thought to affect the flow appreciably (Tyler 2003). Studying the effect of imposing a background magnetic field on a system within a finger regime is therefore somewhat irrelevant to Earth processes. It is nonetheless an interesting phenomena with probable applicability to other planetary bodies.

A second configuration of double-diffusive instability is one in which the temperature gradient is unstable and the compositional gradient is stable, indicating that $\Gamma = \frac{-dT}{dz}$ and $\Gamma = \frac{-d\tilde{S}}{dz}$, so that the system is “top heavy” thermally and “bottom heavy” compositionally. The term describing the advection of vorticity due to buoyancy within the vorticity equation, for such a system is

$$Pr(Ra \frac{\partial T}{\partial x} - \xi Ra_{comp} \frac{\partial C}{\partial x}) \hat{\mathbf{z}} \quad . \quad (0.36)$$

A system described by equation 0.36 diffuses heat quickly but loses a negligible amount of composition, requiring that a fluid parcel displaced upward will quickly become much heavier than its surroundings and sink back down toward its initial position. As the particle approaches its initial position it once again becomes thermally buoyant and the process restarts, producing oscillatory motion. Laboratory experiments show that the initial oscillatory instability does not last long, and eventually results in the formation of a number of horizontal convecting layers, as shown in Fig. 0.4 (Kundu & Cohen 2008). The initial oscillating instability begins near the bottom and begins to grow as heat from the bottom boundary continues to diffuse in. A well mixed layer eventually develops and is capped by a salinity step, a temperature step, and no density step. A thermal boundary layer is formed due to the heat flux through the convective layer, and as the temperature step across the thermal boundary layer becomes larger, the Rayleigh number eventually reaches its critical value. When the critical Rayleigh number is reached another convecting layer develops on top of the first.

The conditions for oscillating instability are present at the boundary of the solid inner and liquid outer core of the Earth. The boundary region develops a strongly unstable compositional gradient as the inner core grows through solidification of the heavy components of the liquid iron alloy in the outer core. Impurities in the alloy, such as sulphur, oxygen and silicon, remain in the fluid of the outer core, generating a source of composition at the interface. This process is considered

to be a source of power for the Earth’s geodynamo, and it is therefore only natural to investigate the effects of a magnetic field on oscillating convective regimes.

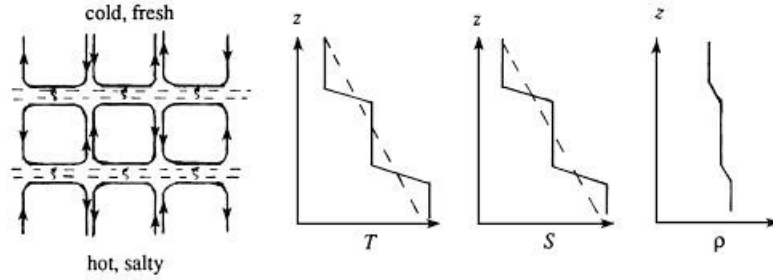


Figure 0.4: Oscillating instability, finally resulting in a series of convecting layers separated by “diffusive” interfaces. Across these interfaces the temperature and composition vary sharply, but heat is transported much faster than composition. (Kundu & Cohen 2008)

3.3

Linear Stability Analysis for Double-Diffusive Regimes

Derivation of the requirement for the onset of instability in double-diffusive regimes is accomplished by generalizing the linear stability analysis of Rayleigh-Bénard convection to include compositional diffusion. The advection-diffusion equations for composition and temperature as described by Eq. 0.31 and 0.9 are identical when making the assumption that $T = \xi C$. Defining the temperature and compositional profiles as such allows for the term describing the advection of vorticity due to buoyancy within the vorticity equation to be written as

$$\pm Pr(Ra \pm Ra_{comp}) \frac{\partial T}{\partial x} \hat{\mathbf{z}}. \quad (0.37)$$

This is identical to the term for the advection of vorticity due to buoyancy within the vorticity equation for Rayleigh-Bénard convection, with $(Ra + Ra_{comp})$ replacing Ra . For the oscillating regime $Ra_{comp} < 0$ and for the finger regime $Ra < 0$. The same analysis of the critical Rayleigh

number for a given aspect ratio in Rayleigh-Bénard convection can be applied here, noting that the compositional Rayleigh number must differ from the thermal Rayleigh number by some distinct value for instability to occur.

Magnetohydrodynamics

In the early 20th century the scientific world became aware of the spontaneous generation of magnetic fields through convection of conducting fluids. Although magnetic fields in nature either originate in certain solids or in convecting, conducting fluids, all studies of magnetic fields prior to this time were with regard to the magnetic properties of solids. The study of the behavior of an electrically conducting fluid in the presence of a magnetic field came to be known as magnetohydrodynamics, and is a topic significant to physics, geophysics, astrophysics, oceanography and engineering.

The approximation that is generally applied to the study of magnetohydrodynamics is one which considers only the low-frequency motions of the electrically conducting fluid considered. Low-frequencies correspond to long wavelengths, indicating that in the low-frequency limit of MHD only the behavior of large scale structure is acknowledged. In the low-frequency approximation one neglects kinetic effects as well as the difference in motion of the various components of the fluid such as the electrons, various kinds of ions, and neutral particles (Polovin 1990). The MHD approximation is quite intuitive when considering that the interference of high and low-frequency processes results in the dampening of the short-wavelength components. A wonderful example (Polovin 1990) is from acoustics —far from an orchestra only the drum is heard. The long-wavelength terms of the relevant quantities can therefore be seen to dominate over long time intervals and at large distances from the source.

4.1

Governing Equations

The motion of a conducting fluid through a magnetic field results in the generation of an electric field and the appearance of electric currents. A magnetic field will alter the motion of an electrically conducting fluid; in turn, the currents induced in the electrically conducting fluid work

to modify the background magnetic field. The equations of magnetohydrodynamics describe such interactions through combination of the equations from electromagnetism and hydrodynamics.

The total force on a particle moving with velocity v and carrying a charge q is generally equal to the sum of three electromagnetic forces,

$$\mathbf{f} = q(\mathbf{E}_s + \mathbf{E}_i + \mathbf{v} \times \mathbf{B}) \quad . \quad (0.38)$$

The individual components represent the electrostatic force (E_s), the force the charge experiences in the presence of a magnetic field (E_i) and the Lorentz force, which arises from the motion of the charge in a magnetic field. Defining the total electric field as $E = E_s + E_i$ allows for the familiar and elegant articulation of Maxwell's equations,

$$\nabla \cdot \mathbf{E} = \frac{\rho_e}{\epsilon_0} \quad (0.39)$$

$$\nabla \times \mathbf{E} = -\frac{\partial \mathbf{B}}{\partial t} \quad (0.40)$$

$$\nabla \times \mathbf{B} = \mu \mathbf{J} \quad (0.41)$$

$$\nabla \cdot \mathbf{B} = 0 \quad (0.42)$$

$$\mathbf{f} = q[\mathbf{E} + (\mathbf{v} \times \mathbf{B})] \quad (0.43)$$

where J is the current density, B is the magnetic field, and ρ_e is the electric charge density.

The total electric field as measured in a frame of reference moving with the conducting fluid is

$$\mathbf{E}_{tot} = \mathbf{E} + \mathbf{v} \times \mathbf{B} \quad . \quad (0.44)$$

The current density is proportional to the force experienced by the free charges, and is given by Ohm's Law

$$\mathbf{j} = \sigma \mathbf{E}_{tot} = \sigma(\mathbf{E} + \mathbf{v} \times \mathbf{B}) \quad ; \quad (0.45)$$

where σ is the fluid's electrical conductivity.

Within the MHD approximation, where we are interested in the bulk force acting on the medium rather than forces on individual charges, it is necessary to sum Eq. 0.43 over the fluid's volume. With $\sum q = \rho_e$ and $\sum q\mathbf{v} = \mathbf{J}$ Eq. 0.43 becomes

$$\mathbf{F} = \rho_e \mathbf{E} + \mathbf{J} \times \mathbf{B} \quad . \quad (0.46)$$

It is assumed that the fluid velocity is non-relativistic, so that terms of order $(\frac{v}{c})^2$ are neglected. Therefore, the electric force density $q\mathbf{E}$ in Eq. 0.46 vanishes, leaving only the Lorentz force contribution.

For a fluid in which σ is considered constant, equations 0.40, 0.41 and 0.42 produce

$$\frac{\partial \mathbf{B}}{\partial t} = \nabla \times (\mathbf{v} \times \mathbf{B}) + \eta \nabla^2 \mathbf{B}. \quad (0.47)$$

Equation 0.47 is the governing equation for the evolution of a magnetic field in a conducting medium and is known as the magnetic induction equation, with $\eta = \frac{1}{\mu\sigma}$ as magnetic diffusivity (where μ is the permeability of free space). If the material is at rest then Eq. 0.47 is limited to the diffusion equation,

$$\frac{\partial \mathbf{B}}{\partial t} = \eta \nabla^2 \mathbf{B} \quad . \quad (0.48)$$

In the limiting case where the fluid has negligible electrical resistance, Eq. 0.47 reduces to

$$\frac{\partial \mathbf{B}}{\partial t} = \nabla \times (\mathbf{v} \times \mathbf{B}) \quad , \quad (0.49)$$

implying that the field behaves as if it were “frozen” into the fluid. Fluid motion along the field lines will not affect the field, but when the material moves transverse to the field lines it will carry them with it (Cowling 1976).

The relationship $\nabla \cdot \mathbf{B} = 0$ invites the introduction of the magnetic vector potential \mathbf{A} ,

$$\mathbf{B} \equiv \nabla \times \mathbf{A} \quad . \quad (0.50)$$

Making use of \mathbf{A} within Eq. 0.49 and carrying out non-dimensionalization through the scaling of \mathbf{B} by B_0 and length, time, and velocity as described by Eq. 0.7 results in

$$\frac{\partial \mathbf{A}}{\partial t} = [-(\mathbf{v} \cdot \nabla) \mathbf{A} + \frac{1}{q} \nabla^2 \mathbf{A}] \quad , \quad (0.51)$$

where $q = \frac{\kappa}{\eta}$ is the Roberts number, defined as the ratio of thermal to magnetic diffusivities.

4.2

Imposing a Background Magnetic Field

The uniform background magnetic field imposed upon the model for Rayleigh-Bénard convection with the inclusion of double-diffusion previously described is restricted to two-dimensions, with only a vertical component initially, such that $\mathbf{B} = B_0 \hat{\mathbf{z}}$. Establishing a magnetic vector potential $\mathbf{A} = A \hat{\mathbf{y}}$ satisfies the condition that the magnetic field is divergence free, and gives the following components for the magnetic field,

$$B_z = \frac{\partial A}{\partial x} \quad \text{and} \quad B_x = -\frac{\partial A}{\partial z} \quad . \quad (0.52)$$

The advection-diffusion equation for the magnetic vector potential now contains only a y-component,

$$\frac{\partial A}{\partial t} = [-(\mathbf{v} \cdot \nabla)A + \frac{1}{q} \nabla^2 A] \hat{\mathbf{y}} \quad . \quad (0.53)$$

Ampere's Law, $\nabla \times \mathbf{B} = \mu \mathbf{J}$, can be used to relate the current density and the magnetic vector potential such that the diffusive term in Eq. 0.53, $\eta \nabla^2 \mathbf{A}$, is equivalent to $\frac{J}{\sigma}$. Using the product rules for vector identities and Eq. 0.52 it can be verified that the advection term in Eq. 0.53, $-(\mathbf{v} \cdot \nabla) \mathbf{A}$, is equal to $(\mathbf{v} \cdot \mathbf{B})_y$.

The boundary conditions instituted upon the magnetic vector potential for this model require that the side boundaries be electrically insulating and the upper and lower boundaries be permeable to the magnetic field. These conditions are mathematically represented by

$$A = 0 \quad \text{at} \quad x = 0 \quad (0.54)$$

$$A = a \quad \text{at} \quad x = a \quad (0.55)$$

and

$$\frac{\partial A}{\partial z} = 0 \quad \text{at} \quad x = 0, L \quad \& \quad z = 0, D \quad (0.56)$$

where a remains as the ratio of the region's length to depth, known as the aspect ratio.

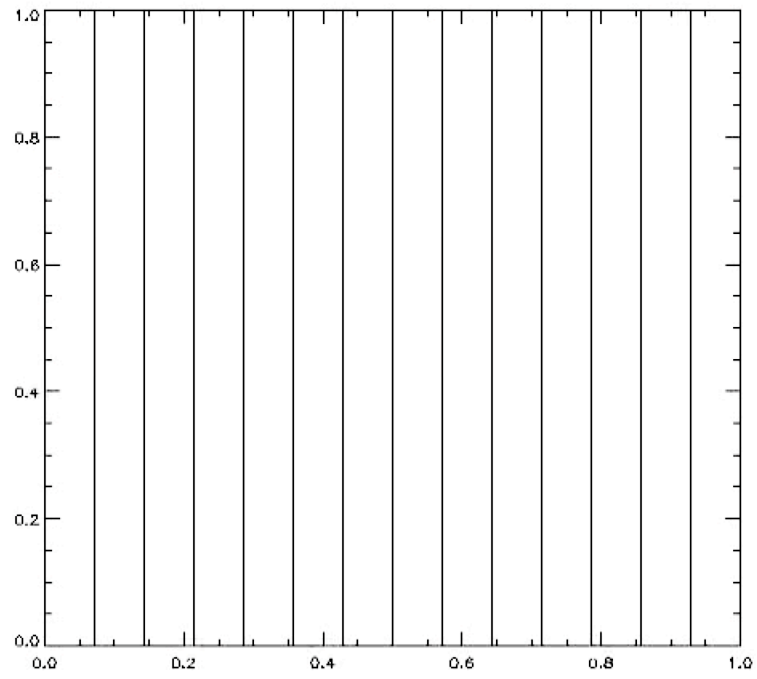


Figure 0.5: A snapshot of the initial magnetic field

Complete Model

The behavior of a conducting fluid within a double-diffusive regime in the presence of a background magnetic field is fully described by the following set of equations.

$$\frac{\partial \omega}{\partial t} = -(\mathbf{v} \cdot \nabla)\omega \pm Pr(Ra \frac{\partial T}{\partial x} \pm Ra_{comp}\xi \frac{\partial C}{\partial x}) + Pr\nabla^2\omega + \frac{QP_r}{q}[(\mathbf{B} \cdot \nabla)J] \quad (0.57)$$

$$\omega = -\nabla^2\psi \quad (0.58)$$

$$\frac{\partial A}{\partial t} = -(\mathbf{v} \cdot \nabla)A + \frac{1}{q}\nabla^2A \quad (0.59)$$

$$\frac{\partial C}{\partial t} = -(\mathbf{v} \cdot \nabla)C + \xi\nabla^2C \quad (0.60)$$

$$\frac{\partial T}{\partial t} = -(\mathbf{v} \cdot \nabla)T + \nabla^2T \quad (0.61)$$

The respective boundary conditions are given by Eq. 0.12 - 0.18, 0.55 and 0.56.

The term $\frac{QP_r}{q}[(\mathbf{B} \cdot \nabla)J]$ is representative of the Lorentz torque, equivalent to the curl of the Lorentz force within the MHD approximation (Eq. 0.46). The inclusion of the Lorentz torque in the vorticity equation follows from the addition of the Lorentz force to the equation of conservation of momentum (Eq. 0.5), a statement of Newton's Second Law, that the mass density times the acceleration is equal to the sum of the forces on the fluid parcel. The ratio of Lorentz to viscous forces, $\Omega = \frac{\sigma B_0^2 D^2}{\rho_0 \eta}$, is the Chandrasekhar number.

6

Numerical Methods

The numerical methods used for code implementation presented here follow the work of Glatzmaier, 2010. Derivatives with respect to time are computed using an explicit Adams-Bashforth scheme, and vertical and horizontal derivatives are approximated using finite difference and horizontal spectral schemes, respectively. The non-linear terms of Eq. 0.57 - 0.61 are expanded in spectral (Fourier) space in a manner similar to the Fourier expansions introduced in the section on linear stability analysis for the Rayleigh-Bénard convection model.

6.1

Time Integration

The time derivatives for the complete model are represented numerically using a second-order accurate linear multistep method known as the Adams-Bashforth explicit time integration scheme. A linear multistep method assumes that the time derivative of the variable considered can be approximated as changing linearly over small periods of time. The Adams-Bashforth method uses the values of the variable at the current and previous time step to extrapolate the time derivative at the mid-point between the current and next time step. The extrapolated value of the variable at the midpoint is then fully advanced to the new time step, and the process is repeated.

The version of the Adams-Bashforth scheme used here computes the time derivative at the mid-point between the previous and current time step by summing the time derivative of the current time step weighted by $\frac{3}{2}$ and the previous time step by $\frac{1}{2}$. If the time derivative of a variable ϵ is defined as

$$\frac{\partial \epsilon}{\partial t}_{t+\frac{\Delta t}{2}} = G_{t+\frac{\Delta t}{2}} \quad , \quad (0.62)$$

then the mathematical representation of the Adams-Bashforth scheme is

$$\frac{\epsilon_{t+\Delta t} - \epsilon_t}{\Delta t} = \frac{3}{2}G_t - \frac{1}{2}G_{t-\Delta t} \quad (0.63)$$

$$\epsilon_{t+\Delta t} = \epsilon_t + \frac{\Delta t}{2}(3G_t - G_{t-\Delta t}) \quad . \quad (0.64)$$

To ensure the accuracy and stability of the Adams-Bashforth method described it is necessary to impose conditions on the size of the time step (Δt) used. The Courant-Friedricks-Lewy (CFL) condition represents advective constraints and states that no fluid particle may travel a distance greater than the grid spacing Δz or Δx in time Δt (Griebel 1998). The CFL condition is mathematically represented by

$$\Delta t < \frac{\Delta z}{|v_z|_{max}} \quad \text{and} \quad \Delta t < \frac{\Delta x}{|v_x|_{max}} \quad . \quad (0.65)$$

In the case of the complete magnetohydrodynamical model it is necessary to include the CFL condition for transverse disturbances in the field (Glatzmaier),

$$\Delta t < \frac{\Delta z}{|v_{Az}|_{max}} \quad (0.66)$$

where v_A is the non-dimensional Alfvén velocity;

$$\mathbf{V}_A = \left(\frac{QPr}{\rho_e} \right)^{\frac{1}{2}} \mathbf{B} \quad . \quad (0.67)$$

The diffusive constraints on the size of the time step require that Δt be less than the time it takes for the thermal perturbation to diffuse over distance Δz ,

$$\Delta t < \frac{(\Delta z)^2}{\kappa} \quad . \quad (0.68)$$

Using methods of non-dimensionalization and considering the magnetohydrodynamical model, Eq. 0.68 reduces to

$$\Delta t < \frac{(\Delta z)^2 \rho_e}{4} \quad . \quad (0.69)$$

6.2

Vertical Finite Difference Discretization

In numerical analysis, the term discretization refers to passing from a continuous problem to one considered at only a finite number of points (Griebel 1998). Discretization represents a given set of differential equations by an approximate system of algebraic equations capable of producing the numerical solution to the original set at a finite number of points on a well-defined domain. The finite difference discretization method is used to represent the vertical derivatives of the complete model.

The easiest way to introduce the finite difference method is by examining the definition of the derivative,

$$\left(\frac{\partial f}{\partial x}\right)_i \equiv \lim_{\delta x \rightarrow 0} \frac{f(x + \delta x) - f(x)}{\delta x} \quad , \quad (0.70)$$

on a one dimensional grid consisting of points $x_i = i \delta x$ where $i = 0 : i_{max}$. Equation 0.70 approx-

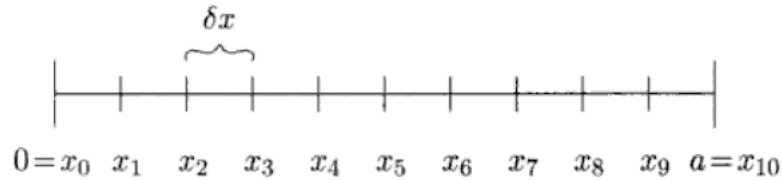


Figure 0.6: A one-dimensional equispaced grid with $i_{max}=10$. (Griebel 1998)

imates the derivative at a grid point x_i using the right neighboring grid point as

$$\left(\frac{\partial f}{\partial x}\right)_i = \frac{f_{i+1} - f_i}{\delta x} \quad , \quad (0.71)$$

The derivative at point x_i is approximated using the left neighboring grid point as

$$\left(\frac{\partial f}{\partial x}\right)_i = \frac{f_i - f_{i-1}}{\delta x} \quad . \quad (0.72)$$

Averaging Eq. 0.71 and 0.72 produces the central difference, and it is this approximation that is

used to compute first derivative at a point x_i

$$\left(\frac{\partial f}{\partial x}\right)_i = \frac{f_{i+1} - f_{i-1}}{2\delta x} \quad . \quad (0.73)$$

The second derivative in the central difference form is computed as the finite difference of Eq. 0.71 and 0.72

$$\begin{aligned} \left(\frac{\partial^2 f}{\partial z^2}\right)_i &= \frac{\left(\frac{\partial f}{\partial x}\right)_{right} - \left(\frac{\partial f}{\partial x}\right)_{left}}{\delta x} \\ &= \frac{f_{i+1} - 2f_i + f_{i-1}}{(\delta x)^2} \quad . \end{aligned} \quad (0.74)$$

6.3

Horizontal Spectral Decomposition

The method of spectral decomposition has already been informally introduced in the section on linear stability analysis. The method of spectral decomposition approximates functions using Fourier expansions, which yields an approximation of the given function as a finite series of sines and/or cosines whose coefficients are sought and must be solved for. This model uses the method of spectral decomposition to represent derivatives in the horizontal direction.

The spectral decomposition of the functions describing the complete magnetohydrodynamical model in accordance with the boundary conditions given by 0.12 - 0.18, 0.55 and 0.56 are

$$T(x, z, t) = \sum_{n=0}^{N_n} T_n(z, t) \cos\left(\frac{n\pi x}{a}\right) \quad (0.75)$$

$$\omega(x, z, t) = \sum_{n=1}^{N_n} \omega_n(z, t) \sin\left(\frac{n\pi x}{a}\right) \quad (0.76)$$

$$\psi(x, z, t) = \sum_{n=1}^{N_n} \psi_n(z, t) \sin\left(\frac{n\pi x}{a}\right) \quad (0.77)$$

$$A(x, z, t) = B_0 x + \sum_{n=1}^{N_n} J_n(z, t) \sin\left(\frac{n\pi x}{a}\right) \quad (0.78)$$

$$B_x(x, z, t) = \sum_{n=1}^{N_n} \frac{\partial A_n}{\partial z} \sin\left(\frac{n\pi x}{a}\right) \quad (0.79)$$

$$B_z(x, z, t) = 1 + \sum_{n=1}^{N_n} \left(\frac{n\pi}{a}\right) A_n \cos\left(\frac{n\pi x}{a}\right) \quad (0.80)$$

and

$$J(x, z, t) = \sum_{n=1}^{N_n} J_n(z, t) \sin\left(\frac{n\pi x}{a}\right) \quad (0.81)$$

6.4

Preparation of Model Equations for Code Implementation

This section briefly introduces how the streamfunction ψ and the nonlinear advective terms of Eq. 0.57 - 0.61 were constructed for numerical analysis.

Assembling the Poisson equation, $\omega = \nabla^2 \psi$, for the relationship between the vorticity and the streamfunction as prescribed by Eq. 0.23 using the spectral expansion of the streamfunction (Eq. 0.77) and the finite difference method for the second derivative of ψ with respect to z produces

$$\omega_i = -\left(\frac{\psi_{i+1} - 2\psi_i + \psi_{i-1}}{(\Delta z)^2} - \left(\frac{n\pi}{a}\right)^2 \psi_i\right) \quad (0.82)$$

Solutions to Eq. 0.82 are computed using the tri-diagonal solver described by William H. Press et. al. in the book “Numerical Recipes”. The initial contour lines of the streamfunction formulated for this model are shown in Fig. 0.7.

The non-linear advective terms of the form $-(\mathbf{v} \cdot \nabla)\epsilon$ can be Fourier expanded as double summations using what is known as a Galerkin method. Here we use the example of the term for the advection of vorticity to convey the purpose and processes of the Galerkin method used to compute all the non-linear advective terms of Eq. 0.57 - 0.61 .

The non-linear term representing the advection of vorticity,

$$-(\mathbf{v} \cdot \nabla)\omega = -\left[v_x \frac{\partial \omega}{\partial x} + v_z \frac{\partial \omega}{\partial z}\right] \quad , \quad (0.83)$$

can be rewritten using Eq. 0.23 and the spectral expansions of ω and ψ as

$$\begin{aligned}
-(\mathbf{v} \cdot \nabla)\omega &= - \sum_{n'=1}^{N_n} \sum_{n''=1}^{N_n} \\
&\quad - \left(\frac{n'\pi}{2a} \right) \frac{\partial \psi_{n''}}{\partial z} \omega_{n'} \left(\sin\left((n'' + n')\left(\frac{\pi x}{a}\right)\right) \right. \\
&\quad \left. + \sin\left((n'' - n')\left(\frac{\pi x}{a}\right)\right) \right) + \frac{\partial \omega_{n'}}{\partial z} \psi_{n''} \left(\sin\left((n'' + n')\left(\frac{\pi x}{a}\right)\right) - \sin\left((n'' - n')\left(\frac{\pi x}{a}\right)\right) \right) \quad . \quad (0.84)
\end{aligned}$$

by recognizing that for each individual summation we seek, as discussed in the section on horizontal spectral decomposition, to solve for Fourier coefficients of the form $[(\mathbf{v} \cdot \nabla)\omega]_n$,

$$-(\mathbf{v} \cdot \nabla)\omega = - \sum_{n'=1}^{N_n} [(\mathbf{v} \cdot \nabla)\omega]_n \sin\left(\frac{n\pi x}{a}\right) \quad . \quad (0.85)$$

Eq. 0.84 can be rewritten as

$$\begin{aligned}
-(\mathbf{v} \cdot \nabla)\omega &= - \frac{\pi}{2a} \sum_{n'=1}^{N_n} \sum_{n''=1}^{N_n} \\
&\quad \left(-n' \frac{\partial \psi_{n''}}{\partial z} \omega_{n'} + n'' \psi_{n''} \frac{\partial \omega_{n'}}{\partial z} \right) \delta_{n''+n',n} \\
&\quad - \left(n' \frac{\partial \psi_{n''}}{\partial z} \omega_{n'} + n'' \psi_{n''} \frac{\partial \omega_{n'}}{\partial z} \right) (\delta_{n''-n',n} - \delta_{n'-n'',n}) \quad (0.86)
\end{aligned}$$

where $\delta_{i,j}$ is the kronecker delta function

$$\delta_{i,j} = \begin{cases} 1 & \text{if } i = j \\ 0 & \text{if } i \neq j \end{cases}$$

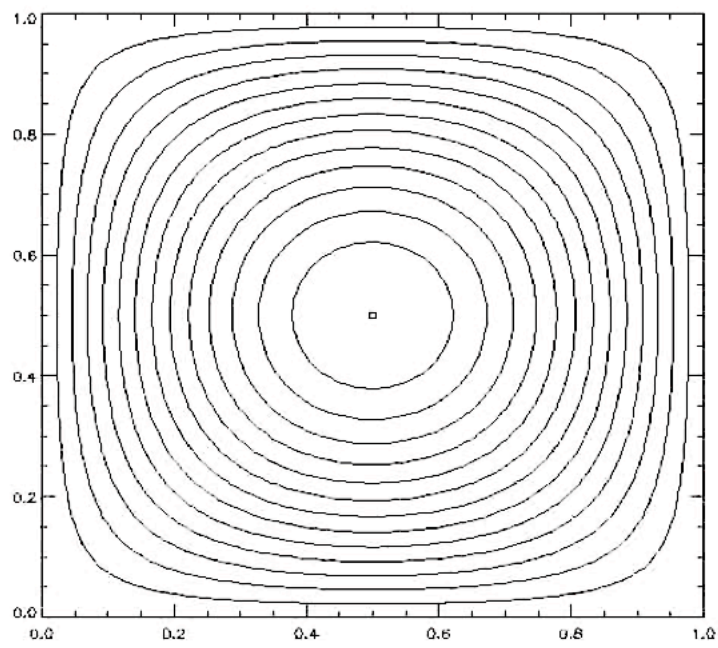


Figure 0.7: Initial contours of the streamfunction

6.5

Code Flow Chart

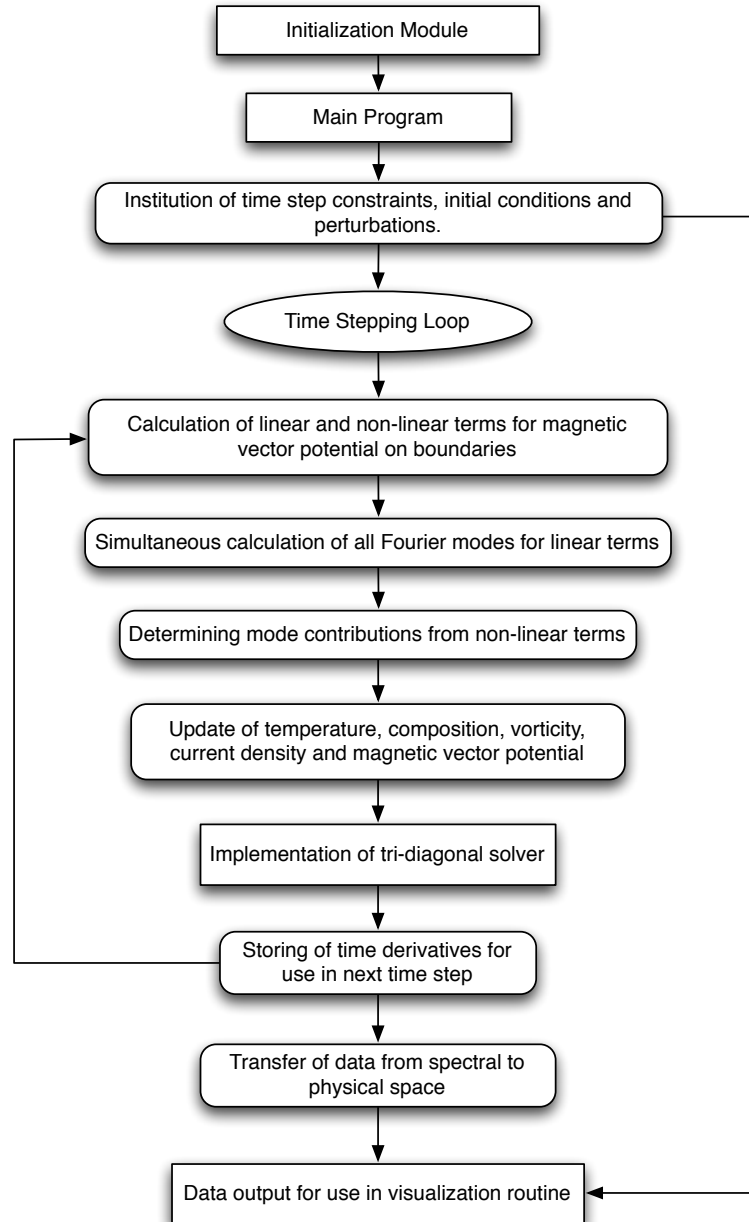


Figure 0.8

Results and Concluding Remarks

This section details the outcome of attempts to simulate two cases of convective instabilities, one in the finger regime and one in the oscillating regime, with varying Chandrasekhar numbers. The analysis of these variations and the subsequent behavior of the system is purely based upon examination of the generated IDL visualizations.

Finger Regime

Table 0.1: Values Chosen for Non-Dimensional Constants

Prandtl Number	0.8
Compositional Rayleigh Number	3×10^7
Thermal Rayleigh Number	-3×10^3
Lewis Number	0.2
Roberts Number	0.2
Aspect Ratio	3

The values in table 0.1 were used for Chandrasekhar numbers of 3×10^2 , 3×10^4 and 3×10^6 . Fingers initially evolved in areas of less magnetic intensity. Increasing the Chandrasekhar number produced thinner fingers which took much longer to develop. For Chandrasekhar numbers of 3×10^2 and 3×10^4 the flow eventually became appreciable enough to eliminate the finger formations and deform the imposed magnetic field. At a Chandrasekhar number of 3×10^6 significant fingers were not formed and the imposed magnetic field was left undeformed, even in simulations run ten times as long as was necessary for well developed finger formation in the simulations with Chandrasekhar numbers of 3×10^2 and 3×10^4 .

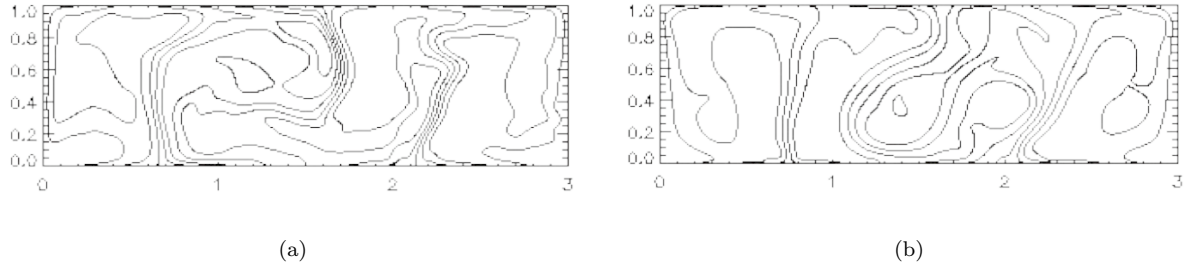


Figure 0.9: Snapshots of the magnetic vector potential contour lines at the final time step for (a) Chandrasekhar number of 3×10^2 . (b) Chandrasekhar number of 3×10^4 .

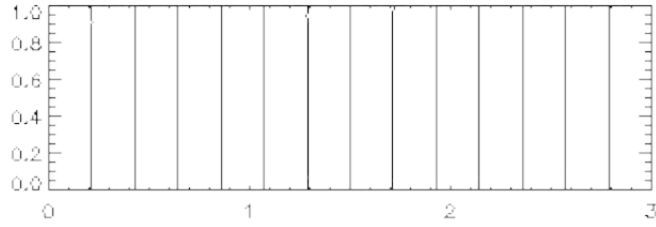


Figure 0.10: Snapshot of the magnetic vector potential contour lines at the final time step for a Chandrasekhar number of 3×10^6 . This simulation was run ten times as long as those for the cases with Chandrasekhar numbers of 3×10^2 and 3×10^4 .

Oscillating Regime

The horizontal layers of convection cells that are characteristic of oscillating regimes were not generated at a level which the author felt was a sufficient representation of the phenomena, and a background magnetic field was therefore not imposed. Simulations varying the effective Rayleigh number ($R_{eff} = R_{thermal} + R_{comp}$ where for the oscillating regime $R_{comp} < 0$), the Lewis number and the aspect ratio were carried out in hopes of catching the oscillating cells represented in Fig. 0.4, but such tactics currently remain fruitless. Neither increasing nor decreasing the level of composition imposed at the bottom boundary produced changes in the initial evolution of the system that led the author to believe that such changes were necessary. Current work is being done to discover

the configuration in which these horizontal layers develop, and the imposition of several different background magnetic fields will provide insight into whether such a seemingly fragile phenomena can develop in the presence of a magnetic field.

The sets of initial values chosen in hopes of generating a system within the oscillating regime are given in table 0.2.

Table 0.2: Values Chosen for Non-Dimensional Constants

Constant	Case 1	Case 2	Case 3	Case 4	Case 5	Case6
Prandtl Number	0.8	0.8	0.8	0.8	0.8	0.8
Compositional Rayleigh Number ($\times 10^6$)	-3	-3	-3	-3	-3	-3
Thermal Rayleigh Number ($\times 10^2$)	3	3	300	300	300	3
Lewis Number	0.2	0.4	0.2	0.2	0.4	0.2
Aspect Ratio	3	3	3	0.8	0.8	0.8

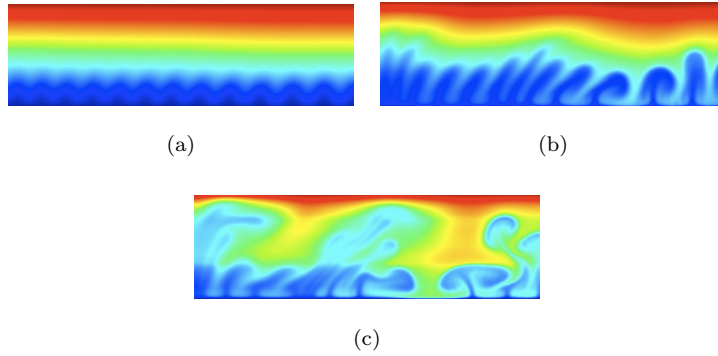


Figure 0.11: Snapshots of composition contour lines for case 2.

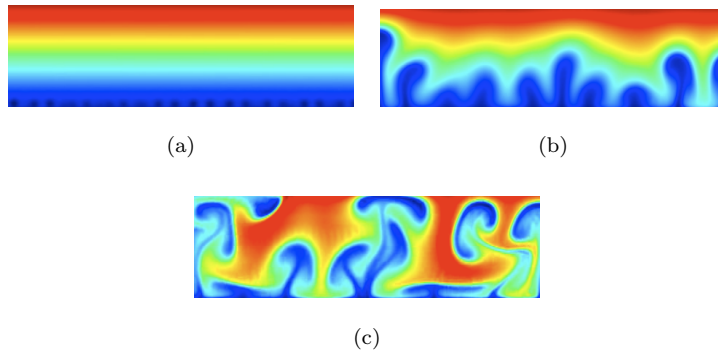


Figure 0.12: Snapshots of composition contour lines for case 3.

Appendix I Complete Fortran 90 Code

```
MODULE data
IMPLICIT none
integer, PARAMETER:: n_z = 100
integer, PARAMETER:: n_n = 100
real*8:: Pr, Ra, aspect, Le, Rc
real*8:: q, F, u
real*8:: pi = 4.*ATAN(1.)
real*8, DIMENSION(n_z) :: z , sub , dia , sup
real*8, DIMENSION(n_z,0:n_n) :: psi , omg , temp, com,.mvp, cur
real, DIMENSION(n_z,0: n_n,1:2) :: domgdt , dtempdt, dcomdt, dcurdt, dmvpdt, dmvpdto, dmvpdtf, b
integer, DIMENSION(2) :: result1 , result2 , result3, result4
integer:: k , n , s , m , p1 , p2 , p3, nsteps
real:: domgdzz , dtempdzz , dpsidzz , domgz , dpsidz , dtempdz, dcomdz, dcomdzz
real*8:: dmvpdzz, dmvpdz, dcurdzz, dcurdz
real*8:: dz , dx , dt , r , c , d , e , dt1, dt2
real:: result11 , result22 , result33, result44
integer:: n_x
real*8, ALLOCATABLE, DIMENSION(:,.) :: phystemp, physpsi, physomg, physcom, physmvp
real*8, ALLOCATABLE, DIMENSION(:,.) :: co, si
real*8, ALLOCATABLE, DIMENSION(:) :: x
```

```
integer :: movstep
character :: movfile*10, movfileid*4, movstr*6, ifmov*1, inst*3
```

```
END MODULE data
```

```
SUBROUTINE error(string)
CHARACTER(LEN=*) :: string
write (*,*) 'error: ',string
STOP 'program terminated by error'
END SUBROUTINE error
```

```
SUBROUTINE tridiag(sub, dia, sup, omg, psi, n_z)
IMPLICIT NONE
integer:: n_z
real, DIMENSION(n_z):: sub, dia, sup, omg, psi
integer:: j,n
REAL, DIMENSION(n_z):: gam,bet

omg(n_z) = 0.
omg(1) = 0.
bet(1) = 1./dia(1)
gam(1) = sup(1)*bet(1)

DO j = 2,(n_z) - 1
bet(j) = 1./(dia(j) - sub(j)*gam(j - 1))
gam(j) = sup(j)*bet(j)
```

```

        END DO

        bet(n_z) = 1./(dia(n_z) - sub(n_z)*gam(n_z - 1))
        psi(1) = omg(1)*bet(1)

        DO j = 2,n_z
            psi(j) = (omg(j) - sub(j)*psi(j - 1))*bet(j)
        END DO

        DO j = n_z - 1,1, - 1
            psi(j) = psi(j) - gam(j)*psi(j + 1)
        END DO
    END SUBROUTINE tridiag

```

```

PROGRAM DDiffMHD
USE data

```

```

write(*,*) 'Enter the number of time steps: '
read (*,*) nsteps
write(*,*) 'Oscillating or finger instability? (osc/fin)'
read (*,*) inst
if (inst .eq. 'osc') then
    write(*,*) 'Ra should be positive and Rac should be negative'
endif
if (inst .eq. 'fin') then
    write(*,*) 'Ra should be negative and Rac should be positive'
endif
write (*,*) 'Enter the Rayleigh number: '
read (*,*) Ra
write (*,*) 'Enter the compositional Rayleigh number: '
read (*,*) Rc
write(*,*) 'Enter the Lewis number: '
read(*,*) Le
write (*,*) 'Enter Prandtl number: '
read (*,*) Pr
write (*,*) 'Enter aspect ratio: '
read (*,*) aspect
write (*,*) ' Enter the Roberts number: '
read (*,*) q
write (*,*) 'Enter the Chandrasekhar number: '
read (*,*) F

```

```

n_x = aspect * n_z

```

```

ALLOCATE ( x(n_x))
ALLOCATE ( co(0:n_n,n_x))
ALLOCATE ( si(0:n_n,n_x))
ALLOCATE ( phystemp(n_x,n_z))
ALLOCATE ( physomg(n_x,n_z))
ALLOCATE ( physpsi(n_x,n_z))
ALLOCATE ( physcom(n_x,n_z))
ALLOCATE ( physmvp(n_x,n_z))

```

```

dz = 1. / float(n_z - 1)
dx = aspect / float(n_x-1)

```

```

dt1 = (0.9)*(dz**2)/4.
dt2 = (dz**2)*q/4.
IF (dt1 .gt. dt2) dt = dt2
IF (dt2 .gt. dt1) dt = dt1
IF (Pr .gt. 1.) dt = dt/Pr
WRITE (*,*) 'Enter the time step dt .le.!',dt,': '
READ (*,*) dt

write(*,*) 'Movie? (y/n)'
read(*,*) ifmov

if (ifmov .eq. 'y') then
  write(*,*) 'how many time steps between movie images?'
  read (*,*) movstep
  write(*,*) 'enter prefix of output files (4 characters)'
  read (*,*) movfileid
endif

```

```

r = (1./dz)**2
c = pi/aspect
u = 1./q
d = 1./(2.*dz)
e = 1./(2.*dx)
sub(2:n_z - 1) = - r
sup(2:n_z - 1) = - r
dia(1) = 1.
sup(1) = 0.
sub(n_z) = 0.
dia(n_z) = 1.

```

```

DO i = 1,n_x
  x(i) = float(i-1) * dx
END DO

```

```

DO n = 0,n_n
  DO i = 1,n_x
    co(n,i) = cos(float(n) * c * x(i))
    si(n,i) = sin(float(n) * c * x(i))
  END DO
END DO

```

```

DO k = 1,n_z
  z(k) = (k-1)*dz
  DO n = 0, n_n
    omg(k,n) = 0.
    psi(k,n) = 0.
   .mvp(k,n) = 0.
    cur(k,n) = 0.
    dcurdt(k,n,1) = 0.
    dcomdt(k,n,1) = 0.
    dtempdt(k,n,1) = 0.
    domgdt(k,n,1) = 0.
    dmvpdt(k,n,1) = 0.
    temp(k,n) = 0.
  END DO
END DO

```

```

    com(k,n) = 0.
  END DO

temp(k,1) = 0.1 * sin(pi*z(k))

  IF (inst .eq. 'osc') THEN
    temp(k,0) = 1. - z(k)
    com(k,0) = z(k)
  END IF

  IF (inst .eq. 'fin') THEN
    com(n_z-1,(n_n/2)+5) = 0.1
    com(n_z-1,(n_n/2)-7) = 0.2
    com(n_z-2,(n_n/2)-11) = 0.2
  ENDIF

  IF (inst .eq. 'fin') THEN
    temp(k,0) = z(k)
    com(k,0) = 1. - z(k)
  END IF

  IF (inst .eq. 'osc') THEN
    com(2,(n_n/2)+5) = 0.1
    com(2,(n_n/2)-7) = 0.2
    com(3,(n_n/2)-11) = 0.2
  ENDIF

END DO

DO s = 0, nsteps
  DO n = 0, n_n
    dmvpdzzo = 2 * (mvp(2,n) - mvp(1,n)) * r
    dmvpdzzf = 2 * (mvp(n_z-1,n) - mvp(n_z,n)) * r
    dpsidzo = 2 * psi(2,n) * d
    dpsidzf = - 2 * psi(n_z-1,n) * d
    dmvpdto(1,n,2) = dpsidzo + u * (dmvpdzzo - ((n*c)**2) * mvp(1,n))
    dmvpdtf(n_z,n,2) = dpsidzf + u * (dmvpdzzf - ((n*c)**2) * mvp(n_z,n))
    cur(1,n) = -(dmvpdzzo - (n * c)**2 * mvp(1,n))
    cur(n_z,n) = -(dmvpdzzf - (n * c)**2 * mvp(n_z,n))
    DO m = 1, n_n
      p1 = n - m
      p2 = n + m
      p3 = m - n

      IF ((p1 .ge. 1) .and. (p1 .le. n_n)) THEN
        dpsidzo = 2 * psi(2,p1) * d
        dpsidzf = - 2 * psi(n_z-1,p1) * d
        dmvpdt(1,n,2) = dmvpdt(1,n,2) - (0.5 * c) * (- m * dpsidzo * mvp(1,m))
        dmvpdt(n_z,n,2) = dmvpdt(n_z,n,2) - (0.5 * c) * (-m * dpsidzf * mvp(n_z,m))
      END IF

      IF ((p2 .ge. 1) .and. (p2 .le. n_n)) THEN
        dpsidzo = 2 * psi(2,p2) * d
        dpsidzf = - 2 * psi(n_z-1,p2) * d
        dmvpdt(1,n,2) = dmvpdt(1,n,2) + (0.5 * c) * (m * dpsidzo * mvp(1,m))
        dmvpdt(n_z,n,2) = dmvpdt(n_z,n,2) + (0.5 * c) * (m * dpsidzf * mvp(n_z,m))
      END IF
    END DO
  END DO

```

```

IF ((p3 .ge. 1) .and. (p3 .le. n_n)) THEN
  dpsidzo = 2 * psi(2,p3) * d
  dpsidzf = - 2 * psi(n_z-1,p3) * d
  dmvpdt(1,n,2) = dmvpdt(1,n,2) - (0.5 * c) * (m * dpsidzo *.mvp(1,m))
  dmvpdt(n_z,n,2) = dmvpdt(n_z,n,2) - (0.5 * c) * (m * dpsidzf *.mvp(n_z,m))
END IF
END DO
END DO

```

```

DO k = 2,(n_z) - 1
  DO n = 0,n_n
    dmvpdzz = (mvp(k+1,n) - 2*mvp(k,n) + mvp(k-1,n)) * r
    dpsidz = (psi(k+1,n) - psi(k-1,n)) * d
    dmvpdt(k,n,2) = dpsidz + u * (dmvpdzz - ((n*c)**2) * mvp(k,n))
    dtempdzz = (temp(k+1,n) - 2 * temp(k,n) + temp(k-1,n)) * r
    dtempdt(k,n,2) = dtempdzz - ((n*c)**2)*temp(k,n)
    dcomdzz = (com(k+1,n) - 2 * com(k,n) + com(k-1,n)) * r
    dcomdt(k,n,2) = Le * (dcomdzz - ((n*c)**2)*com(k,n))
    domgdzz = (omg(k+1,n) - 2 * omg(k,n) + omg(k-1,n)) * r
    dcurdz = (cur(k+1,n) - cur(k-1,n)) * d
    domgdt(k,n,2) = (Ra*Pr*n*c*temp(k,n)) + (Le*Rc*n*c*com(k,n)) + (Pr*domgdzz) -
    (Pr*((n*c)**2)*omg(k,n)) + dcurdz
  END DO

```

```

DO m=1,n_n
  dpsidz = (psi(k+1,m) - psi(k-1,m)) * d
  dtempdz = (temp(k+1,m) - temp(k-1,m)) * d
  dcomdz = (com(k+1,m) - com(k-1,m)) * d
  dcomdt(k,0,2) = dcomdt(k,0,2) - (0.5*c) * m * ((dpsidz*com(k,m)) + (dcomdz*psi(k,m)))
  dtempdt(k,0,2) = dtempdt(k,0,2) - (0.5*c) * m * ((dpsidz*temp(k,m)) + (dtempdz*psi(k,m)))
END DO

```

```

DO n=1,n_n
  dtempdz = (temp(k+1,0) - temp(k-1,0)) * d
  dcomdz = (com(k+1,0) - com(k-1,0)) * d
  dtempdt(k,n,2) = dtempdt(k,n,2) - n*c*psi(k,n)*dtempdz
  dcomdt(k,n,2) = dcomdt(k,n,2) - n*c*psi(k,n)*dcomdz
  DO m = 1,n_n
    p1 = n - m
    p2 = n + m
    p3 = m - n

```

```

    dtempdz = (temp(k+1,m) - temp(k-1,m)) * d
    dcurdz = (cur(k+1,m) - cur(k-1,m)) * d
    domgdz = (omg(k+1,m) - omg(k-1,m)) * d
    dcomdz = (com(k+1,m) - com(k-1,m)) * d

```

```

    IF ((p1 .ge. 1) .and. (p1 .le. n_n)) THEN
      dpsidz = (psi(k+1,p1) - psi(k-1,p1)) * d
      dmvpdz = (mvp(k+1,m) - mvp(k-1,m)) * d
      dmvpdt(k,n,2) = dmvpdt(k,n,2) - (0.5 * c) * (- m * dpsidz * mvp(k,m) + p1 * psi(k,p1) * dmvpdz)

```

```

      dmvpdz = (mvp(k+1,p1) - mvp(k-1,p1)) * d
      b(k,n,2) = 0.5 * c * (- m * dmvpdz * cur(k,m) + p1 * mvp(k,p1) * dcurdz)
      dcomdt(k,n,2) = dcomdt(k,n,2) - (0.5 * c) * (- m * dpsidz * com(k,m) + p1 * psi(k,p1) * dcomdz)

```



```

    dtempdt(k,n,2) = dtempdt(k,n,2) - (0.5 * c) * ( - m * dpsidz * temp(k,m) + p1 * psi(k,p1) *
dtempdz)
    domgdt(k,n,2) = domgdt(k,n,2) - (0.5 * c) * ( - m * dpsidz * omg(k,m) + p1 * psi(k,p1) * domgz)
+ F * Pr * u * b(k,n,2)
    END IF

    IF ((p2 .ge. 1) .and. (p2 .le. n_n)) THEN
        dpsidz = (psi(k+1,p2) - psi(k-1,p2)) * d
        dmvpdz = (mvp(k+1,m) - mvp(k-1,m)) * d
        dmvpdt(k,n,2) = dmvpdt(k,n,2) + (0.5 * c) * (m * dpsidz * mvp(k,m) + p2 * psi(k,p2) * dmvpdz)

        dmvpdz = (mvp(k+1,p2) - mvp(k-1,p2)) * d
        b(k,n,2) = - 0.5 * c * (m * dmvpdz * cur(k,m) + p2 * mvp(k,p2) * dcurdz)
        dcomdt(k,n,2) = dcomdt(k,n,2) - (0.5 * c) * (m * dpsidz * com(k,m) + p2 * psi(k,p2) * dcomdz)
        dtempdt(k,n,2) = dtempdt(k,n,2) - (0.5 * c) * (m * dpsidz * temp(k,m) + p2 * psi(k,p2) *
dtempdz)
        domgdt(k,n,2) = domgdt(k,n,2) + (0.5 * c) * (m * dpsidz * omg(k,m) + p2 * psi(k,p2) * domgz) +
F * Pr * u * b(k,n,2)
    END IF

    IF ((p3 .ge. 1) .and. (p3 .le. n_n )) THEN
        dpsidz = (psi(k+1,p3) - psi(k-1,p3)) * d
        dmvpdz = (mvp(k+1,m) - mvp(k-1,m)) * d
        dmvpdt(k,n,2) = dmvpdt(k,n,2) - (0.5 * c) * (m * dpsidz * mvp(k,m) + p3 * psi(k,p3) * dmvpdz)

        dmvpdz = (mvp(k+1,p3) - mvp(k-1,p3)) * d
        b(k,n,2) = 0.5 * c * (m * dmvpdz * cur(k,m) + p3 * mvp(k,p3) * dcurdz)
        dcomdt(k,n,2) = dcomdt(k,n,2) - (0.5 * c) * (m * dpsidz * com(k,m) + p3 * psi(k,p3) *
dcomdz)
        dtempdt(k,n,2) = dtempdt(k,n,2) - (0.5 * c) * (m * dpsidz * temp(k,m) + p3 * psi(k,p3) * dtempdz)
        domgdt(k,n,2) = domgdt(k,n,2) - (0.5 * c) * (m * dpsidz * omg(k,m) + p3 * psi(k,p3) * domgz) +
F * Pr * u * b(k,n,2)
    END IF

    END DO
    END DO
END DO

DO n = 1,n_n
    mvp(1,n) = mvp(1,n) + (0.5 * dt) * (3 * dmvpdt(1,n,2) - dmvpdt(1,n,1))
    mvp(n_z,n) = mvp(n_z,n) + (0.5 * dt) * (3 * dmvpdt(n_z,n,2) - dmvpdt(n_z,n,1))
END DO

DO k=2,n_z - 1
    temp(k,0) = temp(k,0) + (0.5*dt)*(3*dtempdt(k,0,2) - dtempdt(k,0,1))
    com(k,0) = com(k,0) + (0.5*dt)*(3*dcomdt(k,0,2) - dcomdt(k,0,1))
    DO n = 1,n_n
        com(k,n) = com(k,n) + (0.5*dt)*(3*dcomdt(k,n,2) - dcomdt(k,n,1))
        temp(k,n) = temp(k,n) + (0.5*dt)*(3*dtempdt(k,n,2) - dtempdt(k,n,1))
        omg(k,n) = omg(k,n) + (0.5*dt)*(3*domgdt(k,n,2) - domgdt(k,n,1))
        mvp(k,n) = mvp(k,n) + (0.5*dt)*(3*dmvpdt(k,n,2) - dmvpdt(k,n,1))
    END DO
END DO

DO k = 2,n_z-1
    DO n = 0,n_n
        dmvpdzz = (mvp(k+1,n) - 2 * mvp(k,n) + mvp(k-1,n)) * r
        cur(k,n) = -(dmvpdzz - ((n * c)**2) * mvp(k,n))
    END DO
END DO

```

```
END DO
END DO
```

```
DO n = 1, n_n
  DO k = 2, (n_z) - 1
    dia(k) = ((n*c)**2) + (2.*r)
  END DO
  call tridiag(sub, dia, sup, omg(1,n), psi(1,n), n_z)
END DO
```

```
DO k = 2, n_z - 1
  DO n = 1, n_n
    dcomdt(k,n,1) = dcomdt(k,n,2)
    dtempdt(k,n,1) = dtempdt(k,n,2)
    domgdt(k,n,1) = domgdt(k,n,2)
    dmvpdt(k,n,1) = dmvpdt(k,n,2)
  END DO
END DO
```

```
result11 = maxval(temp)
result22 = maxval(psi)
result33 = maxval(omg)
result44 = maxval(com)
result1 = maxloc(temp)
result2 = maxloc(psi)
result3 = maxloc(omg)
result4 = maxloc(com)
```

```
IF (mod(s,1000)==0) THEN
write(*,*), 'checking maximum amplitudes'
write(*,*), 'time step'
write(*,*), s
write(*,*), 'temperature'
write(*,*), result11
write(*,*), result1
write(*,*),
write(*,*), 'composition'
write(*,*), result44
write(*,*), result4
write(*,*),
write(*,*), 'streamfunction'
write(*,*), result22
write(*,*), result2
write(*,*),
write(*,*), 'vorticity'
write(*,*), result33
write(*,*), result3
write(*,*),
END IF
```

```
DO i = 1, n_x
```

```

DO k = 1, n_z
  phystemp(i,k) = 0.
  physcom(i,k) = 0.
  physpsi(i,k) = 0.
  physmvp(i,k) = 0.
END DO
END DO

IF ((ifmov.eq.'y') .and. (mod(s,movstep).eq.0)) THEN
DO i = 1, n_x
  DO k = 1,n_z
    phystemp(i,k) = temp(k,0)
    physpsi(i,k) = 0.
    physcom(i,k) = com(k,0)
    physmvp(i,k) =.mvp(k,0) + x(i)
    DO n = 1,n_n
      phystemp(i,k) = phystemp(i,k) + temp(k,n) * co(n,i)
      physpsi(i,k) = physpsi(i,k) + psi(k,n) * si(n,i)
      physcom(i,k) = physcom(i,k) + com(k,n) * co(n,i)
      physmvp(i,k) = physmvp(i,k) +.mvp(k,n) * si(n,i)
    END DO
  END DO
END DO

write(movstr, "(i6)") s/movstep
DO ii = 1,6
  if(movstr(ii:ii) .eq. ' ')movstr(ii:ii) = '0'
END DO
movfile = movfileid//movstr(1:6)
open(3,file = movfile, form = 'formatted')
write(3,22), n_x, n_z, aspect, Ra, Pr
22 format(2i7,3(1x,1pe10.3))
DO k = 1, n_z
  write(3,23) (phystemp(i,k),i=1,n_x)
23  format(7(1x,1pe10.3))
END DO
DO k = 1, n_z
  write(3,23) (physpsi(i,k),i=1,n_x)
END DO
DO k = 1, n_z
  write(3,23) (physcom(i,k),i=1,n_x)
END DO
DO k = 1, n_z
  write(3,23) (physmvp(i,k),i=1,n_x)
END DO

close(3)

END IF

END DO

END PROGRAM DDiffMHD

```



```

if N_ELEMENTS(nlevs) ne 0 then begin
    if((nlevs mod 2) eq 0) then nlevs=nlevs+1
endif else begin
    nlevs=15
endelse
amin=0.
amax=1.
if(ifpsi eq 'y') then begin
    amin=min(psi)
    amax=max(psi)
endif
if(ifmvp eq 'y') then begin
    amin=min(mvp)
    amax=max(mvp)
endif
if(N_ELEMENTS(aminmax) ne 0) then begin
    amin=amin-aminmax*(amax-amin)
    amax=amax+aminmax*(amax-amin)
endif
levs=amin+findgen(nlevs)/(nlevs-1)*(amax-amin)
x=findgen(nx)/(nx-1)*aspect
z=findgen(nz)/(nz-1)

    nxwin=480
    nywin=round(nxwin/aspect)
if ((ifcom eq 'y') or (iftem eq 'y')) then begin
    loadct,33
    cr=bindgen(256)
    cg=bindgen(256)
    cb=bindgen(256)
    tvlct,cr,cg,cb,/get
    device,true_color=24
endif

window,1,xsize=nxwin,ysize=nywin,retain=2,/pixmap
mpeg_id=mpeg_open([nxwin,nywin],filename=filename)

while FILE_TEST(file) do begin

    DDiffMHD,file

    if(iftem eq 'y') then begin
        t=congrid(tem,nxwin,nywin,cubic=-0.5,/minus_one)
        t=bytsc1(t,min=t_min,max=t_max)
        t=reverse(t,2)
        y=bytarr(3,nxwin,nywin)
        y(0,*,*)=cr(t(*,*))
        y(1,*,*)=cg(t(*,*))
        y(2,*,*)=cb(t(*,*))
        tv,y,true=1,/order
        write_ppm,file+'.ppm',y
    endif

    if(ifcom eq 'y') then begin
        t=congrid(com,nxwin,nywin,cubic=-0.5,/minus_one)
        t=bytsc1(t,min=t_min,max=t_max)
        t=reverse(t,2)
        y=bytarr(3,nxwin,nywin)
    endif

```

```

y(0,*,*)=cr(t(*,*))
y(1,*,*)=cg(t(*,*))
y(2,*,*)=cb(t(*,*))
tv,y,true=1,/order
write_ppm,file+'.ppm',y
endif

if(ifpsi eq 'y') then $
  contour,psi,x,z,thick=1.5,/isotropic,levels=levs,c_linestyle=2*(levs lt 0.)
if(ifmvp eq 'y') then $
  contour,mvp,x,z,thick=1.5,/isotropic,levels=levs,c_linestyle=2*(levs lt 0.)
mpeg_put,mpeg_id>window=1,frame=count,/order

PRINT,'count=',count
count=count+1
file=STRMID(file,0,nfile-1-(count ge 10)-(count ge 100)- $
(count ge 1000))+STRTRIM(count,2)

endwhile

mpeg_save,mpeg_id
mpeg_close,mpeg_id

end

```

Bibliography

- [1] Cowling, T.G. (1976). *Magnetohydrodynamics*, England: Adam Higler.
- [2] Glatzmaier, Gary (not yet published). *Modeling Convection in Stars and Planets*, Princeton: Princeton University Press.
- [3] Griebel, M., T. Dornseifer and T. Neunhoeffler (1998). *Numerical Simulation in Fluid Dynamics*, Philadelphia: Siam.
- [4] Kundu, P.K and I.M. Cohen (2008). *Fluid Mechanics 4th ed.*, United States: Elsevier.
- [5] Lorrain P., F. Lorrain and S. Houle (2006). *Magneto-Fluid Dynamics: Fundamentals and Case Studies of Natural Phenomena*. New York: Springer.
- [6] Polovin, R.V. and V.P. Demutskii, (1990). *Fundamentals of Magnetohydrodynamics*. New York: Plenum Publishing Corporation.
- [7] Press, W.H. et. al. (1996). *Numerical Recipes in Fortran 90, Vol. 2*, UK: Cambridge University Press.
- [8] Saltzman, Barry (1962). "Finite Amplitude Free Convection as an Initial Value Problem-I." *J. Atmos. Sci.* **19**: 329-341 .
- [9] Taylor, J. and P. Bucens (1989). "Laboratory Experiments on the Structure of Salt Fingers." *Deep-Sea Research* **36**, **11**: 1675-1704 .

- [10] Turner, J.S. (1974). "Double-Diffusive Phenomena." *Annu. Rev. Fluid Mech.* **6**: 37-54 .
- [11] Tyler, R.H., S. Maus and H. Luhr (2003). "Magnetic Fields Due to Ocean Flow." *Science* **299**: 239-299.